05

Investigation of the radiation mode composition of the multimode fiber laser based on measurement of its spectral characteristics

© F.R. Iakupov[1], R.I. Shaidullin[2], A.I. Baranov[3]

[1] Moscow Institute of Physics and Technology (National Research University), Dolgoprudny, Moscow Region, Russia
[2] Kotelnikov Institute of Radio Engineering and Electronics of Russian Academy of Sciences, Fryazino, Russia
[3] OOO „VPG Laserone", Fryazino, Russia
e-mail: iakupov.fr@phystech.edu

Received January 28, 2025
Revised January 28, 2025
Accepted May 05, 2025

The paper presents a method for determining the mode composition of the output radiation of a multimode fiber laser. Since different transverse modes are reflected from a multimode fiber Bragg grating at different wavelengths, then experimental measurement of the optical spectrum of laser radiation allows to determine both the presence of certain modes and the share of optical power in each of them. An experimental study of a multimode fiber laser doped with ytterbium and erbium ions showed that it maintains from 2 to 4 transverse modes depending on the pump power, while the fiber itself supports the propagation of 17 modes.

Keywords: fiber laser, multimode radiation, fiber Bragg grating, optical spectrum.

DOI: 10.61011/EOS.2025.06.61662.7577-25

Introduction

In recent years, fiber lasers and amplifiers in the near-infrared range have gained widespread usage and are actively applied in areas such as material processing, medicine, and telecommunications. Although ideal optical beam quality is achieved only in single-mode (SM) lasers, multi-mode (MM) optical fiber lasers have recently attracted increased interest. This is primarily due to the fact that MM operation allows for higher output power since increasing the fiber core diameter reduces radiation intensity. This makes it possible to increase laser power without triggering various nonlinear effects. Currently, the output power of lasers doped with rare earth ions of ytterbium reaches 10 kW for SM lasers and — for MM lasers. 125 kW [1].

To produce radiation in waveguides with large core diameters but a small number of modes, *LMA* (*large mode area*) fibers are often used [2], where the mode field diameter is increased through special geometry or refractive index profiles of the waveguides. However, even in such fibers, higher-order modes may appear at high radiation powers, and under certain conditions, this can lead to mode instability [3]. Additionally, in high-power optical fiber lasers or amplifiers, there occurs a quasi-static mode degradation effect, where the modal composition and beam quality change over time due to photodarkening [4].

The MM operation of fiber lasers remains poorly understood from a physical perspective, as it becomes necessary to consider multiple transverse modes when describing radiation propagation in the active medium and the transverse distribution of population inversion of active ions. Moreover, the optical radiation quality of MM lasers is noticeably worse and less stable than that of single-mode lasers, making it important to determine the modal composition of the output radiation. This information will allow evaluation of crucial parameters for practical applications, such as beam divergence, transverse intensity profile at different distances from the output fiber end, and minimum focal spot size.

Analysis of the spatial characteristics of output laser radiation most commonly reduces to measuring parameters of the *BPP* (*Beam Propagation Product*) and M^2using various methods. However, these parameters provide a rather crude representation of which modes actually constitute the output radiation. For example, it has been shown that even excellent beam quality ($M^2 < 1.1$) in *LMA* fibers does not guarantee a small number of higher-order modes, and the presence of such modes can lead to significant uncontrolled changes in beam quality and radiation intensity profile [5].

Precise measuring the modal composition of radiation is a highly nontrivial task. From measuring the intensity distribution in the near field, it is possible to calculate the power fraction in two known modes [6], but calculations become drastically more complex for a larger number of modes since the relative phase between modes is unknown. Phases of various modes can be determined using special phase retrieval algorithms applied to measured intensity distributions of the laser beam in the near and far fields [7], or to measured intensity profiles of a collimated beam after a spherical lens [8]. Thus, power distribution among several modes can be obtained. Another method for reconstructing radiation modal composition is based on computer-generated holograms (*CGH*), acting as correlation filters [9]. However, for all the aforementioned techniques, it is necessary to know the set of existing modes in the radiation beforehand.

One of the most well-known methods for obtaining complete information about modes, even in cases of previously unknown radiation modal characteristics and waveguide parameters, is the method based on spatial and spectral resolution of an image obtained from the fiber end (method S^2) [10]. This method is based on the fact that modes propagating in optical fibers can be identified both by group delay difference, which leads to a spectral interference pattern, and by the spatial fringe pattern between a higher-order mode and the main mode. The disadvantage of this method is that it requires the mandatory presence of the fundamental mode LP_{01}, and its power must be higher than that of other modes. In paper [11] proposed improved computational algorithms for the S^2 method, enabling determination of radiation modal composition even with low fundamental mode power. In methods based on S^2, however, it is necessary to use long fiber (up to 20 m) [10] to accumulate group delay between modes, and during propagation through such fiber, the modal composition may change. Another significant limitation is that calculations become significantly more complex as the number of modes increases.

It's important to note that there is a substantial difference between MM radiation propagation in passive fiber and MM radiation generation in active fiber, even if their waveguide characteristics are the same. When several transverse modes propagate in the active fiber core of a fiber laser, the effect of spatial hole burning of population inversion in the active fiber core must be considered [12], as population inversion is depleted more strongly in regions with maximum intensity of that mode's radiation. As a result, population inversion in the transverse section becomes non-uniform. This leads to a reduction in effective gain coefficient for that mode. However, for modes whose maximum intensity occurs in other regions of the transverse section, this effect is less pronounced. Thus, all modes modify the transverse distribution of population inversion and, consequently, gain coefficients both for themselves and for each other. As a result of this modal competition, the laser radiation composition retains only such a set of transverse modes that most effectively depletes population inversion of active ion levels.

Additionally, the laser resonator based on fiber Bragg gratings (FBG) plays an important role. SM FBGs are well-studied from a physical perspective and extensively covered in literature [13]. Their mathematical description uses coupled-mode theory, which has an analytical solution. In contrast, for MM radiation, it becomes necessary to consider multiple transverse modes during reflection [14], complicating the mathematical description of MM FBGs since analytical solutions to coupled-mode equations do not exist in such cases.

Another problem with MM FBGs is the large core diameter, which creates difficulties with the classical UV radiation phase-mask writing method. For example, strong UV absorption in quartz creates a refractive index tilt in the transverse section, complicating calculations [14]. This effect occurs because UV radiation is absorbed in quartz and weakens as it propagates through the section during writing, while refractive index change monotonically depends on UV radiation intensity. This effect leads to modes reflecting from the grating not only into themselves but also into other modes. In paper [15] provides mathematical description of such gratings using coupled-mode theory in the *LP*-mode approximation and proposes a method for finding the reflection matrix of various modes into themselves or each other.

It's important to consider that since transverse mode competition exists in the laser, generation occurs only for a specific set of modes, not for all those supported by the waveguide. This set is determined by the intensity distribution of their electromagnetic fields, feedback coefficient provided by FBGs, and passive radiation losses. Therefore, as stated above, modal composition determination methods based on a pre-known set of modes [6–9] are unsuitable. Application of the S^2 method is possible, though this method is quite complex both experimentally and mathematically. In [15] it was shown that from the reflection spectrum of broadband radiation from an unchirped MM FBG, the modal composition of the incident radiation can be reconstructed, as each transverse mode reflects at a specific wavelength. It is assumed that a similar approach could be used for a laser with a resonator based on such FBGs. It was demonstrated that spectral separation of two transverse modes (LP_{01} and LP_{11}) in a fiber laser on *LMA*-fiber with MM FBG is possible; the possibility of their spatial separation using an external diffraction grating was also shown. An intermediate spectral peak associated with cross-reflection of LP_{01} and LP_{11} modes into each other was also observed. It was demonstrated that the shape of optical signals from a two-mode laser can be adaptively controlled using the FBG transmission/reflection ratio as feedback. Experimentally, it was demonstrated that by maximizing feedback signal at FBG reflection peak wavelength associated with a specific mode LP_{01} or LP_{11}only that single mode can be selectively excited.

The goal of this work is to study the spectral and modal composition of an MM fiber laser assembled from fibers and FBGs investigated in work [15]. To achieve this goal, experimental study of the laser output radiation spectrum was conducted, and modal composition was reconstructed from it at various pumping powers. For qualitative confirmation of the created model's correctness, measurements of transverse intensity distribution of laser output radiation were also performed. An advantage of the method is that modal composition of laser generation is measured directly at the output FBG, and changes in modal composition during propagation through passive fiber do not distort the obtained result. Unlike works [16–18] which studied LMA-fibers where only two transverse modes are excited, standard MM fiber with core diameter 40 μm, supporting a relatively large number (17) of higher-order modes, was investigated.

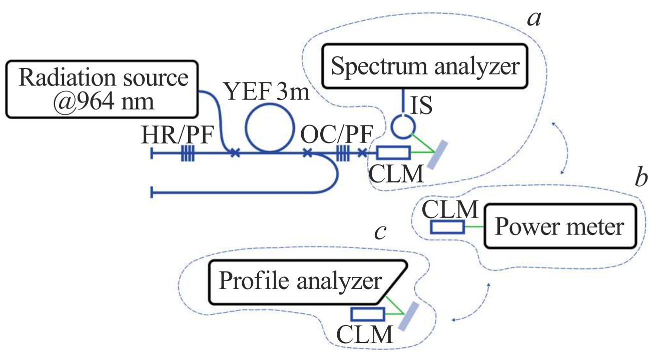

Figure 1. Block diagram of experimental setup and its modifications for: measuring spectral characteristics of output laser radiation (a); measuring output laser radiation power (b); measuring spatial intensity distribution of output laser radiation (c). HR — high-reflection FBG, OC — semi-transparent FBG, PF — passive optical fiber, IS — integrating sphere, CLM — collimator.

Experimental setup

A series of experiments were conducted using an MM fiber laser based on active optical fiber YEF with quartz cladding diameter $125\,\mu$m, core diameter $40\,\mu$m, doped with active ytterbium and erbium ions, and passive optical fiber PF with matching geometric characteristics and mode field diameter. Pumping radiation with wavelength ~ 964 nm was introduced through the passive partYEF, which is a double-clad fiber with side pumping ($DSCCP$) [19]. Semiconductor laser diodes based on GaAs/InGaAs heterostructure served as the pumping radiation source. The FBGs used to create the resonator were written using a phase-mask method on optical fiber PF with period ~ 535 nm. The reflection spectra and parameters of the unchirped semi-transparent FBG (OC) correspond to those obtained in article [15]. The high reflection FBG (HR) was chirped, i.e., had a variable refractive index period along its length, to increase the reflection spectrum width, covering the entire investigated spectral range for all transverse modes. Thus, the spectrum of output laser radiation should be determined only by the parameters of the semi-transparent FBG. A fiber collimator with anti-reflective coating was positioned at the radiation output to reduce beam divergence and minimize back reflections. During laser operation, both FBGs and the active optical fiber were water-cooled for thermal stabilization, as heating causes reflection wavelength shifts. The block diagram of the setup is shown in Fig. 1.

For monitoring spectral characteristics of output laser radiation, a multimode spectrometer Yokogawa AQ6370D was used (Fig. 1, a). Since transverse modes have different spatial intensity distributions when exiting the fiber, the radiation spectral composition will differ at various spatial points. To eliminate dependence of spectrum on radiation propagation direction, an integrating sphere YIXIST XME-2201-02501A-FC was used, which averaged radiation from all modes spatially. Thus, the integral intensity ratio of output fiber laser radiation modes was determined. Radiation was introduced into the sphere using a quartz wedge to attenuate power, with radiation hitting the wedge close to normal incidence to eliminate polarization effects. Multimode optical fiber with core diameter $100\,\mu$m was used as delivery fiber from the integrating sphere to the spectrometer.

For monitoring laser output power, a Coherent Fieldmax II power meter with PM30 sensor head was applied (Fig. 1, b). Maximum laser power reached 12 W at 53 W pumping power.

To qualitatively compare theoretically calculated modal composition with observed spatial intensity profile, a Thorlabs BP-104IR profilometer was used (Fig. 1, c). A quartz wedge was also used to attenuate power during these measurements.

Theoretical Model for Determining Generation Wavelengths of Various LP-Modes

If a multimode FBG is unchirped, i.e., has a constant refractive index period along its length, or if chirp width is small, then spectral lines of reflection for different transverse modes may be resolved. The output FBG (OC) falls into this category. Let's consider the radiation reflection process from such a grating.

Suppose that in mode LP_{mn} the transverse intensity distribution $I_{mn}(z, r, \varphi)$ is given by function $\xi_{mn}(r, \varphi)$, where z is the laser longitudinal coordinate, r and φ are transverse coordinates. Then $I_{mn}(z, r, \varphi) = P(z) \times \xi_{mn}(r, \varphi)$, where $P(z)$ is the power distribution along the longitudinal coordinate. The intensity distribution function satisfies the normalization condition:

$$\int_0^{+\infty}\int_0^{2\pi} \xi_{mn}(r, \varphi) \times r dr d\varphi = 1.$$

Using rate equations approximation, we have [12]:

$$\frac{dP_{mn}}{dz} = P_{mn}\int_0^{+\infty}\int_0^{2\pi}(\sigma_{21}N_2 - \sigma_{12}N_1) \times \xi_{mn} \times r dr d\varphi \Rightarrow$$

$$\frac{P_{mn}(L)}{P_{mn}(0)} = \exp\left\{\int_0^{L}\int_0^{+\infty}\int_0^{2\pi}(\sigma_{21}N_2 - \sigma_{12}N_1) \times \xi_{mn} \times r dr d\varphi dz\right\} \Rightarrow$$

$$G_{mn} = 20\lg(e) \times \int_0^{L}\int_0^{+\infty}\int_0^{2\pi}(\sigma_{21}N_2 - \sigma_{12}(N_0 - N_2) \times \xi_{mn} \times r dr d\varphi dz \Rightarrow$$

$$G_{mn} = 20\lg(e) \times L(\sigma_{21}\bar{N}_{mn} - \sigma_{12}(N_0 - \bar{N}_{mn})). \quad (1)$$

Here $\sigma_{21}(\lambda)$ [m^2], $\sigma_{12}(\lambda)$ [m^2] — are emission and absorption cross-sections of Er active ions, N_2 [m^{-3}] and N_1 [m^{-3}] — are Er active ion concentrations in states $^4I_{13/2}$ and $^4I_{15/2}$, N_0 [m^{-3}] is the total active ion concentration, assumed to be independent of longitudinal and transverse coordinates, G_{mn} [dB] — is the gain coefficient of this LP_{mn}-mode for a full resonator pass, $\bar{N}_{mn}$ is the average population of excited level in active medium for this LP_{mn} mode over longitudinal coordinate and transverse section, L is the active fiber length. Thus, gain factor G_{mn} of this LP_{mn}-mode is determined by the average distribution of excited active ion concentration and radiation wavelength.

Each transverse mode LP_{mn} in the laser generates at the wavelength where the following condition is satisfied with minimal excited level population in the active medium:

$$G_{mn}(\lambda, \bar{N}_{mn}) - A(\lambda, m, n) + R_{OC}(\lambda, m, n) = 0 \quad (2)$$

where λ is emission wavelength, $R_{OC}(\lambda, m, n)$ is the reflection coefficient of mode LP_{mn} at this wavelength in decibels.

We need to specify $A(\lambda, m, n)$. This parameter includes:

1. Resonant cavity passive losses (radiation absorption in quartz, power transfer from this mode to cladding, scattering to surrounding environment at microbends or refractive index inhomogeneities of the optical fiber).

2. Radiation transfer from this mode to other modes at microbends or refractive index inhomogeneities of the optical fiber.

3. Reflection from *HR* grating of radiation from this mode to other modes.

Transferred or reflected radiation into other modes (points 2 and 3) can indeed be considered as losses since at this wavelength *OC* grating effectively reflects only this LP_{mn}-mode. That is, such radiation will not be reflected from the *OC* grating and will leave the resonator.

Within the reflection spectrum of *OC* grating (~ 4 nm) parameter A weakly depends on wavelength. Similarly, parameter G's dependence on wavelength is much weaker than $R_{OC}(\lambda)$'s dependence. Thus, the laser emission wavelength for this LP_{mn} mode is primarily determined by the grating reflection spectrum: emission will occur at the wavelength where reflection coefficient is maximal.

As a first approximation for estimating reflection wavelength of each mode from MM FBG, the phase synchronism condition can be used [15]:

$$\beta_{mn}(\lambda) = \pi/D, \quad (3)$$

where $\beta_{mn}(\lambda)$ is the propagation constant of mode LP_{mn}, determined by solving the boundary problem (wave equation in transverse section of optical fiber), D is the grating period.

A more accurate method for estimating reflection wavelengths of each mode is based on calculating the reflection matrix of OC grating and finding wavelengths corresponding to maximum reflection coefficients for each mode [15]. However, the difference between reflection wavelengths calculated by both methods becomes apparent with large induced refractive index of the grating δn and UV radiation absorption coefficient in quartz μ. In this article, for estimating reflection wavelengths using the second method, induced refractive index was taken as$\delta n = 6 \cdot 10^{-6}$, and tilt parameter, determined by UV radiation absorption coefficient in quartz, as $\mu = 7 \cdot 10^4\,\mathrm{m}^{-1}$. Determination of these values was performed based on analysis of MM FBG reflection spectrum using the method proposed in work [15].

At high laser radiation powers, spatial hole burning effect begins to manifest, leading to the appearance of new transverse modes and consequently spectral components in output radiation.

Theoretical calculations demonstrate [15], that radiation of a specific mode may be reflected from gratings not only into itself but also into another mode. Therefore, a scenario may occur where output laser radiation spectrum contains peaks corresponding to two modes coexisting at the same wavelength, reflecting into each other on both *OC* and *HR* gratings or only on *OC* grating. The reflection wavelength of modes into each other is practically midway between reflection wavelengths of modes reflecting into themselves [15]. No significant changes in the logic of applying equation (2) occur, except that two resonant cavity passes should be considered, where one pass corresponds to one mode, and the second to another mode.

Thus, it has been shown that the generation wavelength of a specific *LP*-mode in an MM fiber laser is primarily determined by the reflection wavelength of the *OC* grating, which can be calculated using two methods.

Discussion of the results

Reflection wavelengths of different modes were determined using two methods described in the previous section: based on phase synchronism condition (3) and based on finding MM FBG reflection matrix using the method described in [15]. The difference in obtained results is much smaller (< 10 pm) than the characteristic peak width (~ 70 pm) in output laser radiation spectra. Complete coincidence of reflection wavelengths obtained from calculations and measured experimentally is not observed due to several reasons: non-ideal grating refractive index profile; grating heating caused by partial absorption of passing radiation; inaccuracy in determining grating parameters, particularly refractive index. When solving the problem of matching calculated wavelengths with experimentally obtained spectral peaks, the following facts must be considered:

1. If mode LP_{01} is present in the output radiation spectrum, it's possible to shift calculated reflection wavelengths so that the longest-wavelength peak in experiment and calculation coincide. According to phase synchronism condition, the fundamental mode reflects at the longest wavelength among all modes. However, as will be shown

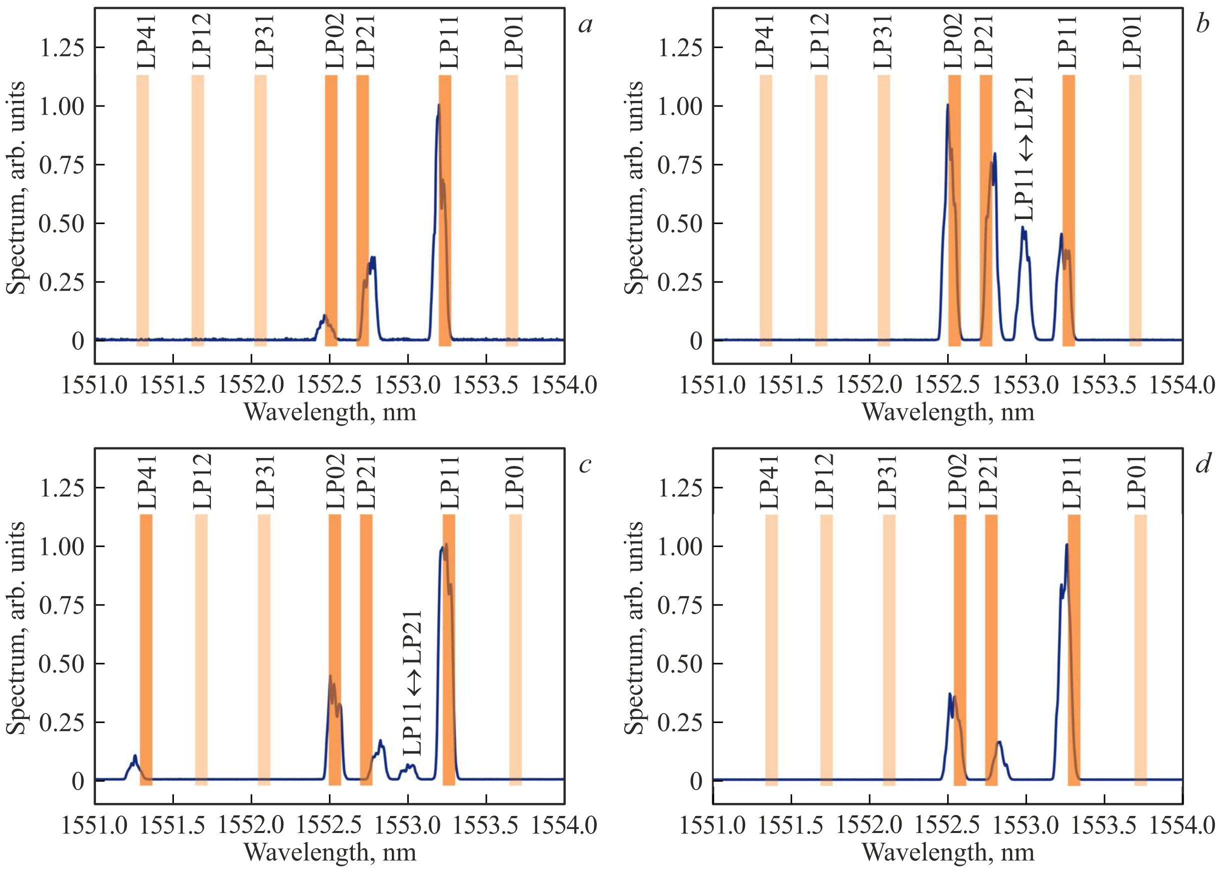

Figure 2. Experimental spectra (blue) obtained for laser pumping powers 6.3 W (*a*), 25.1 W (*b*), 37.4 W (*c*) and 45.6 W (*d*). Orange columns — calculated reflection wavelengths of modes whose width is equal to the width of the peaks in the reflectance spectrum of the grating ($\sim$ 100 pm) [15]. The translucent columns indicate modes that are supported in the fiber but are not implemented during laser generation.

below, mode LP_{01} is absent in output laser radiation in the experiment described in this article.

2. If mode LP_{01} is absent or its presence is unknown, it's possible to analyze distances between various reflection peaks and select a shift so that calculated and experimental peaks coincide with minimal possible deviation.

3. The laser at minimum pump power operates on lower modes. This is because lower modes have larger overlap integral with the active-ion-doped core, i.e., they achieve higher G (1) at the same population inversion in the active medium. Thus, condition (2) for them is satisfied at lower population inversion. As pumping power increases, higher modes appear in the modal composition of output laser radiation due to hole burning effect. Practically, this means that output laser radiation aperture grows with increasing pumping power.

The modal determination algorithm works as follows.

1. In the experimentally obtained output radiation spectrum, peak wavelengths are determined using the algorithm described in [15].

2. Distances between all pairs of experimental peaks are calculated.

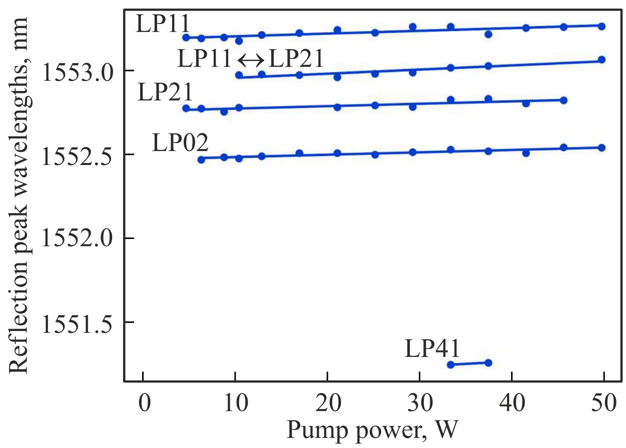

Figure 3. Changes in the reflection wavelengths of experimentally obtained spectral peaks corresponding to different modes as a function of pumping power.

3. A search is performed for coincidences between experimentally determined spectral peak distances and a set calculated based on modeling. The search proceeds from

Table 1. Calculated distances in pm between spectral peaks corresponding to different LP-modes

Mode	LP_{01}	LP_{11}	LP_{21}	LP_{02}	LP_{31}	LP_{12}
LP_{01}	0	430	950	1150	1600	2000
LP_{11}		0	510	730	1180	1580
LP_{21}			0	200	650	1050
LP_{02}				0	450	850
LP_{31}					0	400
LP_{12}						0

Table 2. Mode composition (as a fraction of the output radiation) at different pumping powers

Power of pumping, W	Mode LP_{11}	Mode LP_{21}	Mode LP_{02}	Mode LP_{41}
6.3	0.68	0.24	0.08	0
25.1	0.25	0.38	0.37	0
37.4	0.58	0.11	0.25	0.06
45.6	0.65	0.11	0.24	0

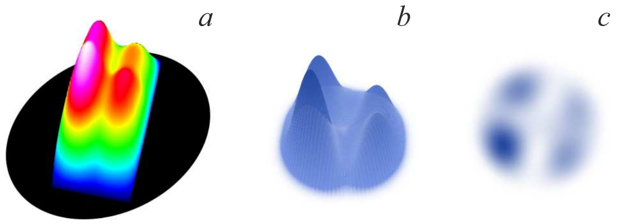

Figure 4. (a) Experimentally measured intensity profile of the laser beam; (b) $3D$-distribution of the calculated intensity profile at a pumping power of 6.3 W (Table 2); (c) $2D$-distribution of the calculated intensity profile at a pumping power of 6.3 W.

lower to higher modes since it's assumed that the laser primarily operates on lower modes first.

Calculated distances in pm between spectral peaks corresponding to various modes are presented in Table 1. The table is symmetric relative to the main diagonal, so only figures for one half are presented.

For example, for the pumping power of 6.3 W, the distance between experimental peaks 1 and 3 is 730 pm, and the distance between experimental peaks 1 and 2 is 440 pm. From the table, it follows that the best match is provided for the following mode combination: peak 1 corresponds to mode LP_{11}, peak 2 to mode LP_{21}, peak 3 to mode LP_{02} assuming peaks correspond to lower modes (Fig. 2, a). Error magnitude equals 70 pm, which coincides with peak width (on average $\sim$ 70 pm) and is smaller than the distance between peaks (more than 100 pm). Error is caused by the resolution of multimode spectrometer when highly-apertured radiation is input, as well as non-ideality of optical fiber PF and MM FBG refractive index profile.

Thus, the proposed algorithm allows determination of the set of modes present in output laser radiation from its spectrum. It can be seen that experimental spectra sometimes contain intermediate peaks corresponding to mode cross-reflection (Fig. 2, b, c), as well as peaks corresponding to higher modes (Fig. 2, c).

It should be noted that experimental peaks and calculated modes can be most easily matched when the number of peaks is no more than 6 but at least 3, and the distance between peaks is large, i.e., at low pumping power. Then, considering that with increasing pumping power, emission wavelengths of modes shift to longer wavelengths due to heating and corresponding refractive index change of FBG, peaks at higher powers where their number is large can be matched with greater reliability. This approach is demonstrated in Fig. 3. Thus, sequential analysis of laser radiation modal composition with gradual increase in laser power allows identification of a larger number of modes realized at high laser radiation power than single measurement at the same power.

Integration of spectra allows determination of power fraction in each transverse mode of output radiation (Table 2).

It is assumed that power of cross-reflection peaks is equally distributed between modes.

To confirm that recovered modal compositions correspond to reality, experimental measurement of transverse intensity profile of the beam at 6.3 W pumping power was performed at 10 mm distance from the collimator using a profilometer (Fig. 1, c). The measurement results are shown in Fig. 4, a. As previously stated, intensity profile doesn't provide complete information about modal composition, so comparison was mostly qualitative. Nevertheless, the characteristic appearance of mode LP_{21}, one of the two main radiation modes, is clearly visible in the experimental beam profile. Calculated intensity profile for modal composition at 6.3 W pump power (Table 2) is presented in Fig. 4, b, c. Thus, good qualitative correspondence between experimental and calculated intensity profiles of output radiation was obtained.

Conclusion

This work presents a new technique for determining the modal composition of MM fiber laser radiation. It has been shown that since different transverse modes reflect from MM FBGs at different wavelengths, experimental measurement of laser radiation optical spectrum allows determination of both presence of specific modes and optical power fraction in each of them.

Investigation of the created fiber laser with active core diameter40 μm showed that 2 to 4 transverse modes are realized depending on power, although the fiber theoretically supports propagation of 17 modes. As power increases, the number of modes generally grows due to spatial hole burning. An unexpected result was the absence of fundamental mode LP_{01}, with most of the power being emitted in modes LP_{11} and LP_{21}. Nevertheless, experimental measurement of spatial intensity distribution in the beam showed qualitative correspondence with calculated modal composition. Additionally, it was found that mode cross-reflection sometimes occurs during reflection from FBGs. This process possibly allows more efficient population inversion depletion in the active core.

Advantages of the presented method over traditional ones include relatively simple experimental measurements and computational model, which allow precise determination of both transverse modes themselves and power fractions in them. Moreover, modal composition is determined at the output MM FBG region and represents direct modal composition of laser generation without distortion in output passive fiber. A significant advantage is that increasing the number of modes doesn't complicate either the experiment or the computational model, only making mode identification more difficult. Sequential analysis of laser radiation modal composition with gradual power increase allows identification of even a large number of modes. A limiting factor is the case when output laser radiation spectrum peaks begin to overlap, making it impossible to match them with specific modes.

Obtained results have high practical significance in MM laser radiation applications. Known modal composition allows determination of key parameters such as laser beam divergence, *BPP* and M^2 parameters characterizing MM fiber laser operation dynamics, focal spot radius, and calculation of radiation intensity profile at required distance from fiber end.

Acknowledgments

The authors thank D.Z. Zubairov (MIPT) for assistance in optical scheme assembly.

Funding

This work was carried out within the framework of the state task of IRE RAS.

Conflict of interest

The authors declare that they have no conflict of interest.

References

[1] IPG Photonics [Electronic source]. URL: https://www.ipgphotonics.com/products/lasers/industrial-cw-fiber-lasers/high-power-fiber-lasers
[2] RP Photonics Encyclopedia [Electronic source]. URL: https://www.rp-photonics.com/large_mode_area_fibers.html
[3] H.-J. Otto, F. Stutzki, F. Jansen, T. Eidam, C. Jauregui, J. Limpert, A. Tünnermann. Opt. Express, **20**, 15710−15722 (2012). DOI: 10.1364/OE.20.015710
[4] L. Xie, C. Zhang, Y. Liu, H. Li, Q. Chu, H. Song, W. Wu, B. Shen, M. Li, X. Feng, S. Huang, R. Tao, J. Wang, X. Zhang, H.Y. Zhu. Opt. Express, **29**, 7986−7997 (2021). DOI: 10.1364/OE.415690
[5] S. Wielandy. Opt. Express, **15**, 15402−15409 (2007). DOI: 10.1364/OE.15.015402
[6] M. Skorobogatiy, C. Anastassiou, S.G. Johnson, O. Weisberg, T. D. Engeness, S. A. Jacobs, R. U. Ahmad, Y. Fink. Opt. Express, **11**, 2838−2847 (2003). DOI: 10.1364/OE.11.002838
[7] O. Shapira, A.F. Abouraddy, J.D. Joannopoulos, Y. Fink. Phys. Rev. Lett., **94**, 143902 (2005). DOI: 10.1103/PhysRevLett.94.143902
[8] D.B.S. Soh, J. Nilsson, S. Baek, C. Codemard, Y. Jeong, V. Philippov. J. Opt. Soc. Am. A, **21**, 1241−1250 (2004). DOI: 10.1364/JOSAA.21.001241
[9] T. Kaiser, D. Flamm, S. Schröter, M. Duparre. Opt. Express, **17**, 9347−9356 (2009). DOI: 10.1364/OE.17.009347
[10] J.W. Nicholson, A.D. Yablon, S. Ramachandran, S. Ghalmi. Opt. Express, **16** (10), 7233−7243 (2008). DOI: 10.1364/oe.16.007233
[11] H.-J. Otto, F. Jansen, F. Stutzki, C. Jauregui, J. Limpert, A. Tunnermann. J. Light. Technol., **31** (8), 1295−1299 (2013). DOI: 10.1109/JLT.2013.2242430
[12] F.R. Iakupov, M.A. Chernikov, A.I. Baranov, R.I. Shaidullin. Appl. Phys. B, **130**, 84 (2024). DOI: 10.1007/s00340-024-08221-0
[13] T. Erdogan. J. Light. Technol., **15** (8), 1277−1294 (1997). DOI: 10.1109/50.618322
[14] C. Lu, Y. Cui. J. Light. Technol., **24** (1), 598−604 (2006). DOI: 10.1109/JLT.2005.859841
[15] F.R. Iakupov, F.V. Zakharov, A.I. Baranov, R.I. Shaidullin. Appl. Phys. B, **131**, 12 (2025). DOI: 10.1007/s00340-024-08373-z
[16] F. Stutzki, C. Jauregui, J. Limpert, A. Tünnermann. Electron. Lett., **47** (4), 274 (2011). DOI: 10.1049/el.2010.3255
[17] F. Stutzki, C. Jauregui, C. Voigtländer, J. Thomas, S. Nolte, J. Limpert, A. Tünnermann. In: *OSA Technical Digest of Optical Fiber Communication Conf.* (Optica Publishing Group, 2010), p. OTuJ2. DOI: 10.1364/OFC.2010.OTuJ2
[18] P. Lu, A. Wang, S. Soker, Y. Xu. Opt. Lett., **40**, 3488−3491 (2015). DOI: 10.1364/OL.40.003488
[19] A.B. Grudinin, D.N. Payne, P.W. Turner, L.J.A. Nilsson, M.N. Zervas, M. Ibsen, M.K. Durkin. U.S. patent 8743454B2 (June 3, 2004).

Translated by J.Savelyeva